


Open Access Article

 <https://doi.org/10.55463/issn.1674-2974.51.5.12>

Seabed Sediment Classification through Multispectral Backscatter Mosaic MBES and Angular Response Analysis

Khomsin^{1,2*}, Mukhtasor¹, Suntoyo¹, Danar Guruh Pratomo²

¹ Ocean Engineering Department, ITS Surabaya, 60111, Indonesia

² Geomatics Engineering Department, ITS Surabaya, 60111, Indonesia

* Corresponding author: khomsin@geodesy.its.ac.id

Received: February 21, 2024 / Revised: March 26, 2024 / Accepted: April 28, 2024 / Published: May 30, 2024

Abstract: Classification of seabed sediments plays a significant role in managing coastal and marine areas. This study aims to classify seafloor sediments in shallow waters using a multispectral backscatter mosaic multibeam echo sounder (MBES) and angular response analysis (ARA), which is validated using in situ sediment data. This research was conducted in the coastal area of Gresik City, East Java, Indonesia, with a depth variation of 3.5–24.5 m. The data utilized consist of multifrequency MBES data collected on January 4, 2023, at frequencies of 400, 300, and 200 kHz. The backscatter data from each frequency is processed to become a backscatter mosaic and merged into a multispectral backscatter. Furthermore, the data were processed using the angular response analysis method to classify the seafloor sediments in the survey area. The classification results were tested using in situ sediment data from a van Veen grab sampler. Sample sediment results were classified based on grain size analysis using the sieving method to determine the sediment type. The results showed that the backscatter mosaic of each frequency and the backscatter multispectral mosaic did not differ visually. However, regarding the backscatter values, there is a difference of about ± 1 dB between frequencies. The foreshore area (western part) and the area farthest from the foreshore (eastern part) show the hard layers identified by the light backscatter mosaic. The ARA classification results revealed six sediment classes in the survey area, which is different from the four types of sediment found in situ. Sediment classification using ARA demonstrated an accuracy rate of 51% for real sediment samples, with a kappa coefficient of 0.3, indicating a fair level of categorization. This implies that half of the expectation point rises to the real test point.

Keywords: seabed sediment, classification, backscatter, mosaic, multispectral backscatter, angular response analysis, overall accuracy, kappa coefficient.

通过多光谱后向散射马赛克微波辐射计和角响应分析进行海底沉积物分类

摘要：海底沉积物分类在管理沿海和海洋区域方面发挥着重要作用。本研究旨在使用多光谱后向散射马赛克多波束回声测深仪(微波辐射计)和角度响应分析(阿拉)对浅水区的海底沉积物进行分类，并使用现场沉积物数据进行验证。这项研究是在印度尼西亚东爪哇省 Gresik 市沿海地区进行的，深度变化为3.5-

24.5米。所用的数据包括2023年1月4日收集的多频率微波辐射计数据，频率为400、300和200千赫。每个频率的后向散射数据被处理后向散射马赛克并合并为多光谱后向散射。此外，使用角度响应分析方法处理数据以对调查区域的海底沉积物进行分类。使用来自范维恩抓

取采样器的现场沉积物数据测试分类结果。使用筛分法根据粒度分析对样品沉积物结果进行分类以确定沉积物类型。结果表明，各频率的后向散射马赛克图和后向散射多光谱马赛克图在视觉上没有差异。然而，就后向散射值而言，频率之间存在约 ± 1 dB的差异。滨海区域（西部）和距离滨海最远的区域（东部）显示出光后向散射马赛克识别的硬层。阿拉分类结果显示，调查区域有六种沉积物类型，与现场发现的四种沉积物类型不同。使用阿拉对沉积物进行分类对真实沉积物样本的准确率为51%，卡帕系数为0.3，表明分类水平相当。这意味着一半的预期点上升到真实测试点。

关键词：海底沉积物，分类，后向散射，镶嵌，多光谱后向散射，角度响应分析，总体精度，卡帕系数。

1. Introduction

Coastal areas are transitional between terrestrial and marine ecosystems that are affected by changes in land and sea. Coastal regions are the most populous and busiest in major cities worldwide. Therefore, disaster mitigation is essential for reducing disaster risk in coastal areas. This involves implementing structural and physical measures, both natural and artificial, and non-structural approaches. Coastal mapping is the first step in learning, managing, protecting, and conserving biodiversity. One of the essential pieces of information needed during coastal mapping, in addition to sea depth, is the mapping of seabed sediments [1]. Seabed sediments can be mapped by mechanical, optical, electromagnetic, and acoustic methods. The mechanical method involves the use of a grab sampler and core, while the optical method utilizes a camera and video. The electromagnetic method relies on satellite remote sensing, and the acoustic method employs the single-beam echo sounder (SBES), side-scan sonar (SSS), sub-bottom profiler (SBP), and multi-beam echo sounder (MBES) [2, 3].

MBES is the most widely used acoustic method for mapping bathymetry and seafloor sediment surveys. The advantages of MBES over other acoustics, such as SBES, SSS, and SBP, include high resolution, swath coverage, and wide depth range. There are currently three main functions of MBES: bathymetry, backscatter, and water column [4]. For sediment mapping, MBES generates three types of data: backscatter mosaic, backscatter angular response, and bathymetry [5]. A backscatter mosaic is a georeferenced image produced by a MBES that displays the acoustic intensity scattered off the seafloor [6]. It can be used to categorize habitats and comprehend prospective environmental changes because different seafloor types typically exhibit varying intensities [7, 8]. Backscatter angular response

[9] quantifies the acoustic intensity scattered from the seabed upon the impact of an acoustic signal from a MBES. The intensity of the scattered acoustic signals varies depending on the angle of the incident signal [10]. The backscatter angular response shows this variation, making it useful for studying seabed sediment. Bathymetry measures the depth of a body of water, such as an ocean, sea, lake, or river. This is different from topography, which measures the shape of the land or ground surface. Bathymetry is important in marine science [11] because it helps researchers track changes in ocean depth and observe how different currents and patterns interact in different parts of the ocean.

Seafloor sediment classification techniques have been developed in the last two decades by exploiting the MBES backscatter feature. The monochromatic backscatter mosaic gray level (high and low intensity) has been extensively used as a feature in many classification techniques [11, 12]. Angular range analysis is a classification technique for signal-based backscatter that has been developed to automatically predict seabed sediment characterization using acoustic inversion [13]. According to [14], the backscatter mosaic and angular response should be combined to obtain the former's satisfactory spatial resolution and the latter's predictive power. Farihah et al. [15] applied backscatter and angular response analysis to detect, classify, and estimate the bottom watershed. Fahrulian et al. [16] analyzed seabed types using angular range analysis (ARA) based on backscatter values. In addition, [17] used ARA to classify seafloor sediments in deep seas using MBES backscatter data. The classification performed by these researchers was unsupervised classification that had no control over the sediment data in situ. In general, it is performed in deep seas; thus, it is difficult to retrieve data in situ. In addition, the backscatter data from the MBES are currently single frequency, encompassing both low and

high frequencies.

Most MBESs operate at a single frequency (monochromatic) analogous to a single waveform in an optical satellite system. This would limit the resolvability of terrestrial land cover features compared to collecting data across a broad spectrum of spectral bands. Therefore, the acquired backscatter is still monochromatic. Wider operating bandwidths have been made possible by advancements in MBES transducer technology, with some systems on the market being able to span several hundred kHz to provide better range resolution for bathymetric data collection [18]. MBES multispectral backscatter data are needed to meet the demand related to improving the accuracy of seafloor sediment classification for habitat and geological mapping purposes, as is the case with remote sensing satellites. For this reason, the latest MBES technology is proposed, which can collect data at several frequencies at one time and at different times. Using MBES multispectral backscatter will likely improve the classification of seafloor sediments [19, 20].

Accordingly, this study aims to classify seabed sediments in shallow waters using multispectral MBES data. The classification method utilized was supervision classification, with seabed sediment in situ serving as the ground-truth information necessary for interpreting the imagery and identifying substrates. The methods used were mosaic multispectral backscatter analysis and angular response analysis. Therefore, the accuracy of sediment classification results will be determined by comparing the use of monospectral and multispectral data through angular response analysis.

2. Materials and Methods

2.1. Research Area

Fig. 1 shows a map where a multifrequency MBES survey was carried out in the shallow coastal water. The location is the PT. Gresik Jasa Tama (PT. GJT) port in Gresik Regency, East Java Province, Indonesia. The PT. GJT port serves as a hub for loading and unloading wooden ships. The MBES bathymetric survey was conducted on Wednesday, January 4, 2023, with a survey area of approximately 41 ha. The survey area depth ranged from approximately -3-m to -25-m LWS. The landforms in the survey region were straightforward, with a conventional harbor and coast. The location chosen for this research object is particularly important because it represents shallow coastal water. The seafloor is covered by various landforms and sediments, including clay, silt, sand, and gravel. Seabed sediments greatly benefit the study of acoustic sediment characterization in this area.



Fig. 1 Research survey area at PT. Gresik Jasa Tama, Gresik Regency, East Java, Indonesia (The authors)

2.2. Multispectral Backscatter MBES Acquisition

Acquisition of backscatter multispectral data used a multifrequency R2Sonic 2020 MBES. The MBES transducer was mounted on the side of the ship for the setting survey. R2Sonic 2020 is a MBES that operates on a ping-by-ping basis, allowing the collection of data across multiple frequencies in a single survey. This survey uses five frequency modes: 200, 250, 300, 350, and 400 kHz. The data acquisition system is set automatically, including the transmission power, gain, and pulse length. An inertial motion unit (IMU) sensor measures the ship's movement, i.e., pitch, roll, and yaw. The heading and horizontal positioning are determined by GNSS differentials directly linked to the CORS station. A sound velocity profiler (SVP) is also included in the survey to measure the velocity of sound waves in the water layer at the start, middle, and end of the survey. SVP data are used to correct the speed of sound waves emitted by the MBES. In addition, tidal observations were also carried out around the location to correct the benchmark to the chart datum, the lowest water surface (LWS). The specifications of the R2Sonic 2020 MBES are listed in Table 1.

Table 1 The R2Sonic 2020 MBES specifications used during data acquisition [21]

Frequency	200–450 kHz; optional 700 kHz
Beam width (Ω_{ix} and Ω_{ix})	$1^\circ \times 1^\circ$ at 700 kHz (optional); $1.8^\circ \times 1.8^\circ$ at 450 kHz; $4^\circ \times 4^\circ$ at 200 kHz
Sounding pattern	Equiangular and equidistant modes, including single, double, and quad, are part of the ultra-high-density (UHD) technology.
Pulse type	Shape CW
Selectable swath sector	The user can select a range of 10° to 130° in real time.
Number of soundings	Up to 1024 soundings per ping
Nominal pulse length τ_n	15 μ s–1 ms

Once all MBES systems are installed correctly, the next step is calibrating the MBES holder using a patch test due to misalignment of the sonar head in the

presence of motion sensors and gyros. Fig. 2 [22] displays the orientation of the R2Sonic MBES head, which is essential for converting the measured slant ranges into depths and specifying each determined depth position. Any error in the sonar head can cause significant errors in the conversion from the slant range to depth.

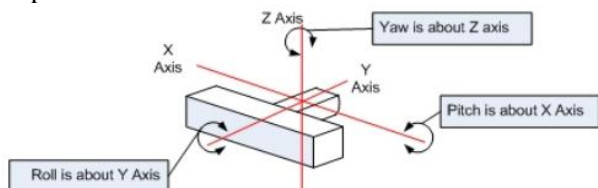


Fig. 2 The R2Sonic 2020 MBES series axes of rotation [22]

A patch test [22] is a calibration procedure used to measure the angular misalignment between the MBES transducer and the ship attitude, i.e., pitch, roll, and yaw. The pitch test was conducted on a steep slope or a seafloor object, while the roll test was performed on a flat seafloor area. The survey was conducted in a single lane, moving back and forth at a consistent speed. Following the pitch and roll tests, the yaw test was carried out in two parallel lines with the same direction along those lines. These lines were positioned either over a slope or the side of a seafloor feature. The value of the patch test, SVP data, and tidal data were entered into each survey data line to correct the data. The raw data must be separated to obtain data for each frequency and then edited to remove noise. Each set of frequency data was processed to create bathymetry, monospectral, and multispectral backscatter mosaics. Seabed sediment characterization was conducted through the use of ARA, which is controlled by in situ sediment data to ensure accuracy in the calculations.

2.3. Seabed Sediment Samples in Situ

Prior knowledge of the seafloor is required to obtain representative seabed sediment samples in a research area. First, bathymetric maps, tidal current knowledge, and other data can provide direction. This preliminary survey can aid in choosing sampling areas before a sampling plan is created. The sediment data were collected from 84 sample locations distributed uniformly throughout the study region (Fig. 3). For biological, hydrological, and environmental investigations in deep water and strong currents, sampling with van Veen's grab is suitable for obtaining bulk samples of a variety of materials, from soft and fine-grained to sandy materials [23]. The sample point position was measured by GNSS RTK with an accuracy of less than 10 cm. The sediment samples underwent sieve analysis to determine the percentage composition of gravel, sand, clay, and silt.

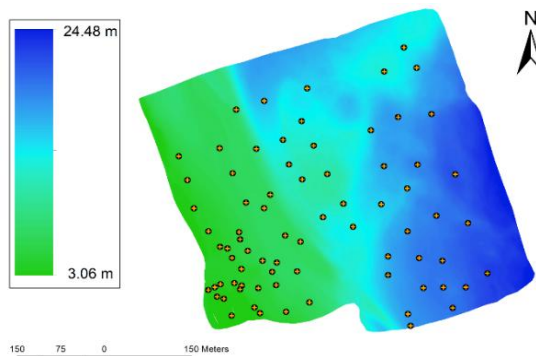


Fig. 3 Seabed sediment sample distribution in the survey area (black dots) (The authors)

3. Results and Discussion

3.1. Digital Bathymetric Model (DBM)

The ship's attitude was corrected using raw data from the R2Sonic 2020 MBES bathymetry by computing the test patch values, namely pitch, roll, and yaw, for each rotation against the x-axis, y-axis, and z-axis, respectively. Then, the data were cleaned from noise caused by reflections from non-seabed objects, such as fish, seaweed, wrecks, and other features. Depth data is corrected to vertical datum, namely the LWS with tidal observation data. To create a digital bathymetric model with a 1-m resolution, the depth data is gridded using kriging, as shown in Fig. 4.

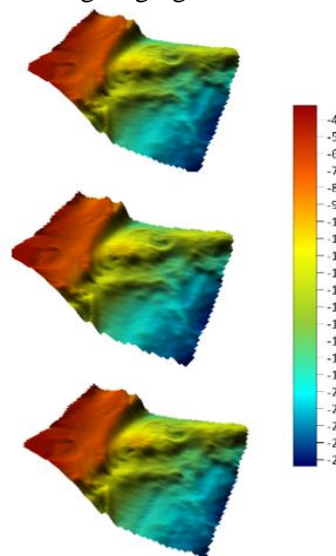


Fig. 4 Digital bathymetric area survey model: 400 kHz (upper), 300 kHz (middle), and 200 kHz (lower) (The authors)

Fig. 4 shows the appearance of the seabed in the survey area at each frequency; 400 kHz, 300 kHz, and 200 kHz were almost the same. The depth in the survey area ranged from -3.5-m LWS to -24.5-m LWS. The western side of the port pool along the coast is shallow, measuring less than -8-m LWS (red). Furthermore, the area in the middle (yellow-green) has a depth between -8-m LWS and -17-m LWS, which is the entrance channel to the port pool. Light blue-dark blue in the

eastern part is the Surabaya West Shipping Channel (APBS), which has a depth of less than -17-m LWS. On the border between the port pool and the channel leading to the pool, there is a cliff with a depth of -7-m to -12-m LWS (red-yellow). The southern part of the survey area is a valley (channel) with a depth range of -14-m to -20-m LWS.

3.2. Sediment Grain Size Analysis

Seventy-four seabed sediment sample points (Fig. 3) were tested in the laboratory using the sieve analysis method. Sieve analysis [24] is used to examine and measure the size of particles in material samples. It typically involves screening a sample through a series of sieves, each of which has a mesh of different size to allow particles of different sizes to pass through. The distribution of particles across various size ranges can be quantified and compared, aiding in the assessment of sample quality. Fig. 5 shows an example of the results obtained using the sieve analysis, with the percentages of gravel (0.0%), sand (12.21%), and mud (fines: silt 78.11% and clay 9.69%).

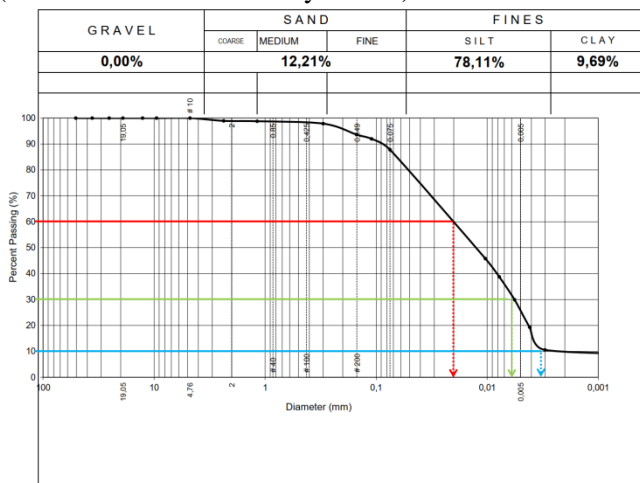


Fig. 5 Grain-size distribution curve (The authors)

Furthermore, the results of the sieve analysis revealed the sediment size percentage composition of each sample, as illustrated in Fig. 5. The classification of the samples was done using a ternary diagram, as depicted in Fig. 6 [25]. The sediment classification at the sample point was sandy silt. The same method was used to classify the other sediment samples.

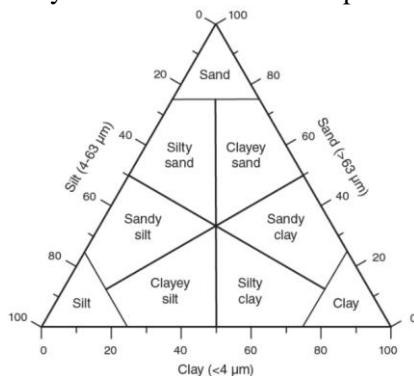


Fig. 6 Ternary diagram showing sediment classification according

to granular texture [25]

Out of the 74 sediment sample points within the survey area, four sediment classes were identified based on ternary diagrams: clayey sand, sandy silt, silt, and silty sand. Furthermore, the data for the sediment type points (x, y, z), where z is the sediment type, were collected to analyze sediment distribution through interpolation techniques. Fig. 7 illustrates the distribution of seafloor sediments in the survey region using linear interpolation.

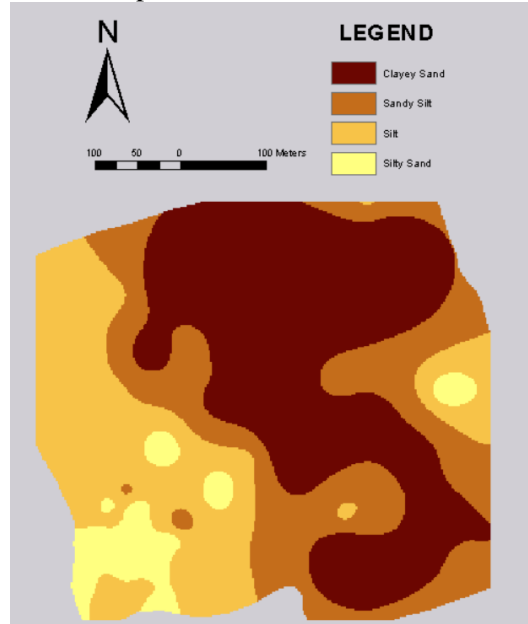
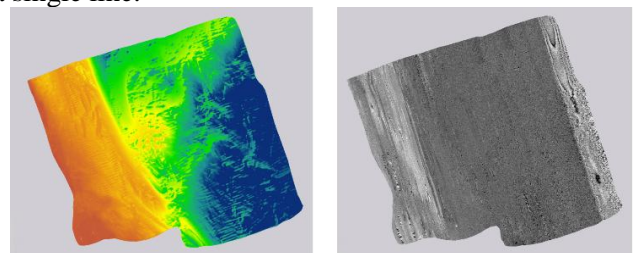


Fig. 7 Seabed sediment classification using in situ sediment samples (The authors)

3.3. Monospectral and Multispectral Backscatter Mosaics

A backscatter mosaic [26] is a digital representation of the seafloor generated from raw signal amplitude data gathered by a multibeam sonar. This visualization is created through software that eliminates disruptive elements like time-varying gain and applies radiometric corrections to produce an image of the seafloor at a resolution of 1.0 m. The mosaic can then be used for further analysis. Fig. 8 shows bathymetric and backscatter mosaic data at frequencies of 400, 300, and 200 kHz. The backscatter results showed that data density is essential for multispectral backscatter analysis and that the data differ from those gathered in a single line.



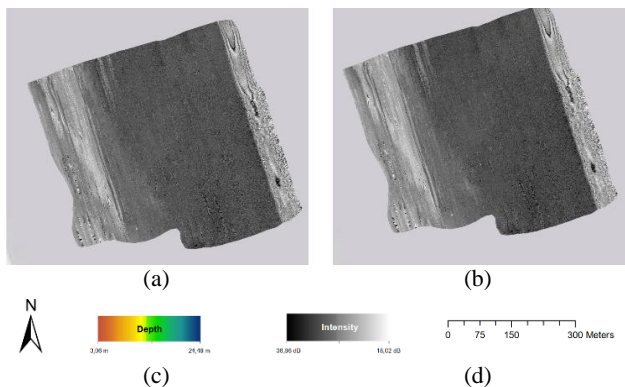


Fig. 8 (a) Bathymetry and monospectral backscatter data collected using MBESs at (b) 200, (c) 300, and (d) 400 kHz (The authors)

Fig. 8(b), (c), and (d) show the backscatter mosaics at frequencies of 400, 300, and 200 kHz, respectively. Generally, the study area's seafloor surface has almost the same intensity for all three frequencies. The light color indicates a higher intensity of -25 dB, and the black indicates an intensity of less than -25 dB. The variation in intensity is attributed to the depth of the area being surveyed. Shallower depths result in higher intensity readings. The survey conducted in the western part of the area exhibited a greater intensity than the readings taken in the middle. In addition, the difference in intensity can also be due to the type of sediment present at the bottom. The density of the seafloor material affects the reflectiveness of the sound waves used in backscatter analysis by MBESs. When the material is denser, such as gravel, sand, or shell, it will produce a stronger signal on the sounder. However, when dealing with materials of lower density, such as mud, clay, and silt, sound waves will penetrate partially into the small grain-sized particles. This leads to a decrease in signal strength.

Furthermore, the backscatter mosaics in Fig. 8 are integrated to form a multispectral backscatter image. Multispectral backscatter [27] is the utilization of multiple frequencies or wavelengths during data collection. This research uses multiple frequencies with a MBES system to collect bathymetry and backscatter data. These data can be utilized to analyze seafloor composition, including hardness, sediment characteristics, and grain size, to differentiate between sediment types. Backscatter mosaics for each frequency in Fig. 8(b), (c), and (d) are overlaid on each other to create multispectral imagery. A multispectral image is captured by a sensor that detects light across various spectrums or frequencies.

Multispectral images are valuable tools for conducting coastal surveys as they offer higher resolutions due to their shorter wavelengths. This enables researchers to detect even the most minor features of the seabed. Multispectral images offer a wealth of information beyond what can be captured by

regular monospectral images, which are limited to capturing light within a single spectrum. Fig. 9 displays a false-color composite featuring various bands (red, green, and blue combinations) for multispectral backscatter mosaics, including RGB234, RGB243, RGB324, RGB342, RGB423, and RGB432, where 4, 3, and 2 correspond to frequencies of 400, 300, and 200 kHz, respectively.

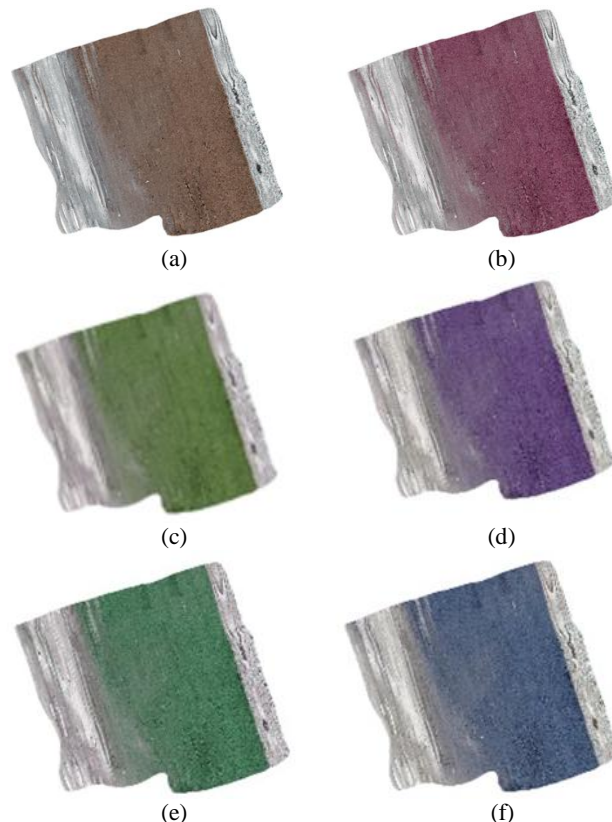


Fig. 9 Multispectral backscatter mosaics: (a) RGB234, (b) RGB243, (c) RGB324, (d) RGB342, (e) RGB423, and (f) RGB432 (The authors)

A false-color composite image is a modified image in which colors have been altered to enhance the identification of various features. This technique is commonly utilized in studies to distinguish between different types of seafloor sediment. For instance, this research utilized false-color composite images to differentiate between hard and soft sediments. The false-color image utilizes three distinct spectral bands, or frequencies, and adjusts their intensities to create a color palette. This makes it easier for researchers to quickly recognize features in images. The three bands refer to three different frequencies that were used to improve our understanding of seafloor geological characteristics and benthic habitats.

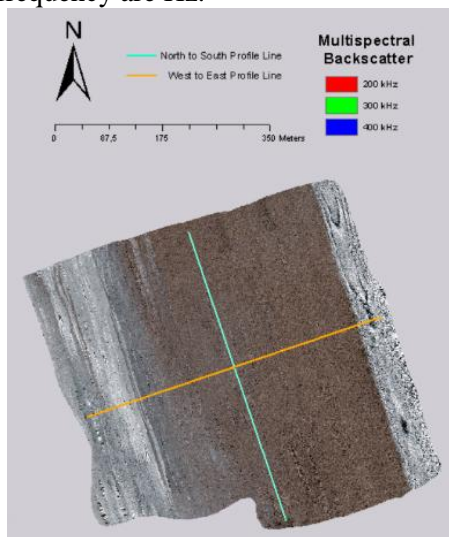
The researchers aimed to distinguish between various types of seafloor substrate and enhance their habitat mapping by integrating these frequencies. For example, when all three frequency bands had equal intensity, the resulting image appeared white, which typically indicates hard seafloor. In contrast, the image

appears black when all three bands are continuously low; this typically occurs in flat places with thick, soft silt layers. Other hues, such as purple, can be produced by variations in the relative intensities of the frequency bands, and this may occasionally reveal information about the types of seafloor substrate.

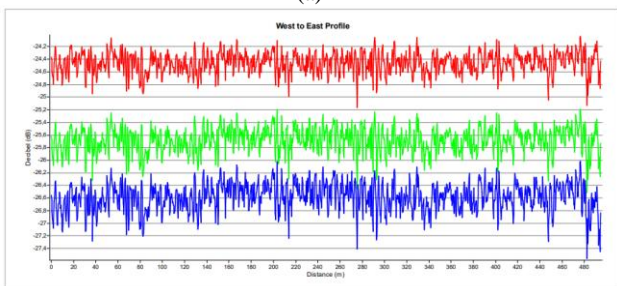
Fig. 10 shows the backscatter intensities from west to east (W-E) and from north to south (N-S). The 200-kHz frequency has a higher intensity than the others because at the same time, depth, and location, the greater the frequency, the greater the attenuation. The relationship between attenuation and frequency is a phenomenon in which a signal's strength decreases as its frequency increases. Simply put, it is the weakening of a signal with an increase in frequency; the amount of attenuation due to scattering increases roughly following a frequency-squared relationship. As the sound wave frequency increases, the attenuation also increases significantly. The scattering attenuation α_s as a function of frequency is [28]:

$$\alpha_s = A_s \times 20 \log_{10} e \times f^2 \quad (1)$$

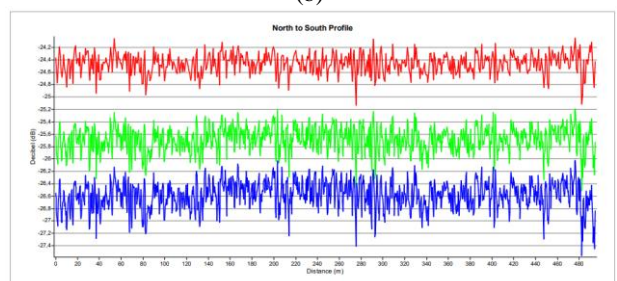
where α_s is the attenuation scattering factor, and the units of frequency are Hz.



(a)



(b)



(c)
Fig. 10 Comparison of the variations in backscatter strength among the multispectral mosaics within the survey location. Backscatter intensities from the three multispectral mosaics are compared along the transect, as indicated in (a) RGB234, (b) from west to east, and (c) from north to south (The authors)

3.4. Seabed Sediment Classification by Angular Response Analysis

Angular range analysis (ARA) is a technique that can be used to calculate the whole angular response curve (ARC) throughout each half of the MBES swath to evaluate substrate attributes [13]. To gain a deeper understanding of the seafloor composition in the region, [26] highlighted the use of ARA as a method for measuring and analyzing sound backscattering from the seafloor. Information is gathered from various angles, and the variance in backscattering with the angle aids in classifying and describing the seafloor. Six types of sediment are shown in the image based on the angular response curve and angular response analysis of backscatter mosaics at frequencies of 400, 300, and 200 kHz: silty sand, clayey sand, sandy silt, clayey silt, sandy clay, and silty clay. The number of ARA classification classes in Fig. 11 differs from the number of in situ sediment data classification classes in Fig. 7.

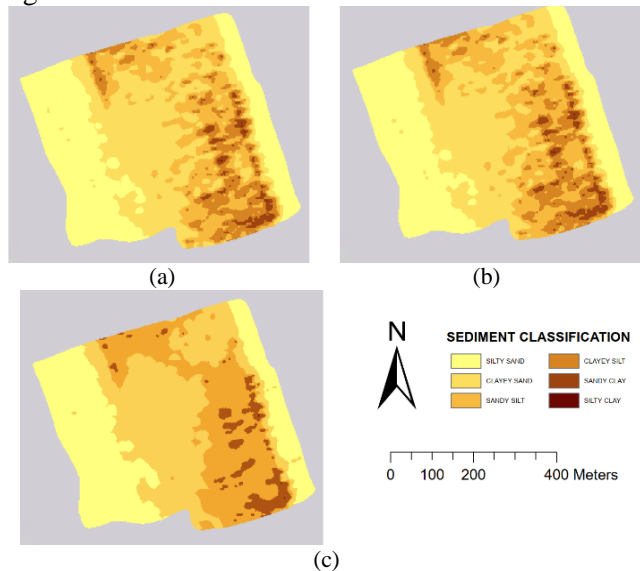


Fig. 11 Seabed classification by the ARA method: (a) 200, (b) 300, and (c) 400 kHz (The authors)

In Fig. 11, this classification of sediments by ARA for each frequency results in a similar seabed sediment distribution. The yellow to the east and west of the survey area indicates the sand class (medium sand–fine sand–silty sand). It aligns with the white backscatter mosaic shown in Fig. 8 and the multispectral backscatter mosaic shown in Fig. 9, indicating the area's highest backscatter value. In the middle of the survey area, silt sediments are dominant (coarse silt–sandy silt–medium silt). A small portion of the area consists of silty clay and clay, as indicated by brown.

The seabed sediment classification using the ARA

method was then tested using 74 sediment sample points spread evenly in the survey area, as shown in Fig. 7. The confusion matrix test [29] can be used to calculate the overall accuracy and kappa coefficient. The classification accuracy measure is a metric that evaluates the accuracy of a classification model. It is calculated by comparing the predictions from the model with the actual classes of the data. High classification accuracy means that the model can accurately predict the data classes. The kappa value is a measure of the accuracy of a predictive model. It varies from 0 to 1, where 0 indicates that the model is completely inaccurate and 1 indicates perfect accuracy. A total of 74 sites in the survey region were used to classify the seabed sediment using the ARA method, which was regulated by the type of sediment. The results show an overall accuracy of 51% and a kappa coefficient of 0.37 for all frequencies. This means that only half of the prediction point is equal to the actual sample point. According to [30], the kappa coefficient of 0.37 belongs to the fair category.

4. Conclusion

For frequencies of 400, 300, and 200 kHz, the backscatter strength in the survey area varied from -36 to -18 dB. In this case, although a frequency of 200 kHz has a backscatter strength that is ± 1 dB higher than that of 300 kHz, a frequency of 300 kHz has a backscatter strength that is ± 1 dB higher than that of 400 kHz, the multispectral backscatter mosaic RGB band configuration in this instance displays the same texture pattern.

The classification of seafloor sediments in coastal areas with a depth of less than 25 m using multifrequency MBES data showed that classification using the angular response analysis (ARA) method resulted in six classes. In general, the distribution of sediments in the form of sand is located to the east and west. The silt class dominates in the middle, and a small part of the area shows the clay class. Each of the frequencies shows a similar classification. Seabed sediment classification using ARA in the survey area with 74 sediment sample points showed an overall accuracy of 51% and kappa coefficient of 0.37.

The results of this study demonstrate the accuracy of the classification of seabed sediments in shallow waters (less than 25 m) using the ARA method, namely the fair category. Enhancing the precision of seabed sediment classification in shallow waters can be achieved by incorporating additional data, such as bathymetry, in addition to backscatter data. These data can then be processed using other methods such as neural networks.

Acknowledgments

We express our gratitude to our colleagues at PT. APBS for their insight and expertise that significantly contributed to the research on the R2Sonic 2020 multi-frequency MBES survey. Additionally, we extend our thanks to Eiva Corporation for providing the Geomatics Engineering Department with licenses for the Navi Edit JobPlanner and Navi Model Producer software.

References

- [1] MAXIM L. D. *Nautical chart user's manual*. 1st ed. National Oceanic and Atmospheric Administration, 1997. <https://repository.library.noaa.gov/view/noaa/49555>
- [2] FONSECA L., & CALDER B. Geocoder: an efficient backscatter map constructor. *U.S. Hydrographic Conference*, 2005. <https://scholars.unh.edu/ccom/339/>
- [3] ZHENG H. B., YAN P., CHEN J., and WANG Y. L. Seabed sediment classification in the northern South China Sea using inversion method. *Applied Ocean Research*, 2013, 39: 131-136. <https://doi.org/10.1016/j.apor.2012.11.002>
- [4] COLBO K., ROSS T., BROWN C., and WEBER T. A review of oceanographic applications of water column data from multibeam echosounders. *Estuarine, Coastal and Shelf Science*, 2014, 145: 41-56. <https://doi.org/10.1016/j.ecss.2014.04.002>
- [5] CHE-HASAN R., IERODIACONOU D., LAURENSEN L., and SCHIMMEL A. Integrating Multibeam Backscatter Angular Response, Mosaic and Bathymetry Data for Benthic Habitat Mapping. *PLoS ONE*, 2014, 9(5): e97339. <https://doi.org/10.1371/journal.pone.0097339>
- [6] LE BAS T. P., & HUVENTE V. A. I. Acquisition and processing of backscatter data for habitat mapping – Comparison of multibeam and sidescan systems. *Applied Acoustics*, 2009, 70: 1248–1257. <https://doi.org/10.1016/j.apacoust.2008.07.010>
- [7] SAMSUDIN S. A., & HASAN R. C. Assessment of multibeam backscatter texture analysis for seafloor sediment classification. *The International Archives of the Photogrammetry, Remote Sensing and Spatial Information Sciences*, 2017, 42: 177-183. <https://doi.org/10.5194/isprs-archives-XLII-4-W5-177-2017>
- [8] BROWN C. J., BEAUDOIN J., BRISSETTE M., and GAZZOLA V. Setting the stage for multi-spectral acoustic backscatter research. *Geological Survey of Canada, Open File*, 2017, 8295: 41. <https://doi.org/10.4095/305838>
- [9] CLARKE J. E. H., DANFORTH B. W., and VALENTINE P. Areal seabed classification using backscatter angular response at 95 kHz. Proceedings of the Conference “High Frequency Acoustics in Shallow Water,” Lerici, 1997, pp. 243–250. http://hydrometrica.com/wp/wp-content/uploads/HFSW_1997_Lerici.pdf
- [10] APPLIED PHYSICS LABORATORY. *APL-UW High-Frequency Ocean Environmental Acoustic Models Handbook*. Applied Physics Laboratory, University of Washington, Seattle, Washington, 1994. <https://staff.washington.edu/dushaw/epubs/APLTM9407.pdf>
- [11] WILSON M. F. J., O'CONNELL B., BROWN C., GUINAN J. C., and GREHAN A. J. Multiscale Terrain Analysis of Multibeam Bathymetry Data for Habitat Mapping on the Continental Slope. *Marine Geodesy*, 2007, 30(1-2): 3–35. <https://doi.org/10.1080/01490410701295962>

- [12] EDWARDS B. D., DARTNELL P., and CHEZAR H. Characterizing benthic substrates of Santa Monica Bay with seafloor photography and multibeam sonar imagery. *Marine Environmental Research*, 2003, 56: 47–66. [https://doi.org/10.1016/S0141-1136\(02\)00324-0](https://doi.org/10.1016/S0141-1136(02)00324-0)
- [13] FONSECA L., & MAYER L. Remote estimation of surficial seafloor properties through the application Angular Range Analysis to multibeam sonar data. *Marine Geophysical Research*, 2007, 28: 119-126. <https://doi.org/10.1007/s11001-007-9019-4>
- [14] FONSECA L. E., & CALDER B. R. Clustering Acoustic Backscatter in the Angular Response Space. *U.S. Hydrographic Conference*, 2007, 384. <https://scholars.unh.edu/ccom/384>
- [15] FARIHAH R. A., MANIK H. M., and HARSONO G. Measurement and Analysis of Acoustic Backscatter Using Multibeam Echosounder Technology for Sediment Classification of the Gulf of Palu. *Jurnal Ilmu dan Teknologi Kelautan Tropis*, 2020, 12(2): 437-453. <https://doi.org/10.29244/jitkt.v12i2.28465>
- [16] FAHRULIAN F., MANIK H. M., JAYA I., and UDREKH U. Angular Range Analysis (ARA) and K-Means Clustering of Multibeam Echosounder Data for Determining Sediment Type. *ILMU KELAUTAN: Indonesian Journal of Marine Sciences*, 2016, 21(4): 177-184. <https://doi.org/10.14710/ik.ijms.21.4.177-184>
- [17] PRATOMO D. G., KHOMSIN, CAHYADI M. N., AKBAR K., and APRILIA E. Analysis of Seafloor Sediment Distribution using Multibeam Backscatter Data. *MATEC Web of Conferences*, 2018, 177: 01026. <https://doi.org/10.1051/mateconf/201817701026>
- [18] LAMARCHE G., & LURTON X. Recommendations for improved and coherent acquisition and processing of backscatter data from seafloor-mapping sonars. *Marine Geophysical Research*, 2018, 39(1): 5-22. <https://doi.org/10.1007/s11001-017-9315-6>
- [19] GAIDA T. C., ALI T. A. T., SNELLEN M., SIMKOOEI A. A., VAN DIJK T. A. G. P., and SIMONS D. G. A Multispectral Bayesian Classification Method for Increased Acoustic Discrimination of Seabed Sediments Using Multi-Frequency Multibeam Backscatter Data. *Geosciences*, 2018, 8(12): 455. <https://doi.org/10.3390/geosciences8120455>
- [20] BROWN C. J., BEAUDOIN J., BRISSETTE M., and GAZZOLA V. Multispectral multibeam echo sounder backscatter as a tool for improved seafloor characterization. *Geosciences*, 2019, 9(3): 126. <https://doi.org/10.3390/geosciences9030126>
- [21] R2SONIC. *Multibeam Echosounder Specifications*, 2020. <https://r2sonic.com/wp-content/uploads/2020/03/MBES-Spec-US-03-02-2020.pdf>
- [22] BRENNAN C. W. Multibeam Calibration: The Patch Test. *R2Sonic*, 2017. <https://r2sonic.com/wp-content/uploads/2020/03/The-New-Patch-Test.pdf>
- [23] INTERNATIONAL ATOMIC ENERGY AGENCY. *Collection and Preparation of Bottom Sediment Samples for Analysis of Radionuclides and Trace Elements*. IAEA, Vienna, 2003. <https://www.iaea.org/publications/6674/collection-and-preparation-of-bottom-sediment-samples-for-analysis-of-radionuclides-and-trace-elements>
- [24] RETSCH. *Sieve analysis: taking a close look at quality. An expert guide to particle size analysis*. 2015. <https://www.retsch.ru/files/8785/expert-guide-sieving.pdf?ysclid=lxj4gres950003340>
- [25] FRANCE-LANORD C., SPIESS V., KLAUS A., ADHIKARI R. R., ADHIKARI S. K., BAHK J.-J., BAXTER A. T., CRUZ J. W., DAS S. K., DEKENS P., DULEBA W., FOX L. R., GALY A., GALY V., GE J., GLEASON J. D., GYAWALI B. R., HUYGHE P., JIA G., LANTZSCH H., MANOJ M. C., MARTOS MARTIN Y., MEYNADIER L., NAJMAN Y. M. R., NAKAJIMA A., PONTON C., REILLY B. T., ROGERS K. G., SAVIAN J. F., SCHWENK T., SELKIN P. A., WEBER M. E., WILLIAMS T., and YOSHIDA K. Site U1452. In: FRANCE-LANORD C., SPIESS V., KLAUS A., SCHWENK T., and THE EXPEDITION 354 SCIENTISTS. *Bengal Fan. Proceedings of the International Ocean Discovery Program*, 354. International Ocean Discovery Program, College Station, Texas, 2016. <http://dx.doi.org/10.14379/iodp.proc.354.106.2016>
- [26] LURTON X., & LAMARCHE G. (eds.) *Backscatter Measurements by Seafloor-Mapping Sonars: Guidelines and Recommendations*, 2015. <https://geohab.org/wp-content/uploads/2018/09/BWSG-REPORT-MAY2015.pdf>
- [27] COSTA B. Multispectral Acoustic Backscatter: How Useful Is It for Marine Habitat Mapping and Management? *Journal of Coastal Research*, 2019, 35(5): 1062–1079. <https://doi.org/10.2112/JCOASTRES-D-18-00103.1>
- [28] WANG J., LI G., KAN G., HOU Z., MENG X., LIU B., LIU C., and LEI S. High frequency dependence of sound speed and attenuation in coral sand sediments. *Ocean Engineering*, 2021, 234: 109215. <https://doi.org/10.1016/j.oceaneng.2021.109215>
- [29] CUNNINGHAM M. More Than Just the Kappa Coefficient: A Program to Fully Characterize Inter-Rater Reliability between Two Raters. *Proceedings of the SAS Global Forum*, 2009. <http://support.sas.com/resources/papers/proceedings09/242-2009.pdf>
- [30] LANDIS J. R., & KOCH G. G. The measurement of observer agreement for categorical data. *Biometrics*, 1977, 33: 159-174. <https://doi.org/10.2307/2529310>

参考文献:

- [1] MAXIM L. D. 海图用户手册。第1版。美国国家海洋和大气管理局，1997年。 <https://repository.library.noaa.gov/view/noaa/49555>
- [2] FONSECA L., & CALDER B. 地理编码器：一种高效的反向散射图构造器。美国水文会议，2005年。 <https://scholars.unh.edu/ccom/339/>
- [3] ZHENG H. B., YAN P., CHEN J., 和 WANG Y. L. 使用反演方法对南海北部海床沉积物进行分类。应用海洋研究，2013年，39：131-136。 <https://doi.org/10.1016/j.apor.2012.11.002>
- [4] COLBO K., ROSS T., BROWN C. 和 WEBER T. 多波束回声测深仪水柱数据的海洋学应用综述。河口、

- 沿海和陆架科学, 2014年, 145 : 41-56. <https://doi.org/10.1016/j.ecss.2014.04.002>
- [5] CHE-HASAN R.、IERODIACONOU D.、LAURENSEN L. 和 SCHIMEL A. 整合多波束后向散射角响应、马赛克和水深测量数据以进行底栖栖息地测绘。公共科学图书馆, 2014年, 9(5) : e97339. <https://doi.org/10.1371/journal.pone.0097339>
- [6] LE BAS T. P. 和 HUVENNE V. A. I. 获取和处理用于栖息地测绘的后向散射数据-多波束和侧扫系统的比较。应用声学, 2009年, 70 : 1248-1257. <https://doi.org/10.1016/j.apacoust.2008.07.010>
- [7] SAMSUDIN S. A. 和 HASAN R. C. 对多波束后向散射纹理分析在海底沉积物分类中的评估。国际摄影测量、遥感和空间信息科学档案, 2017年, 42 : 177-183. <https://doi.org/10.5194/isprs-archives-XLII-4-W5-177-2017>
- [8] BROWN C. J.、BEAUDOIN J.、BRISSETTE M. 和 GAZZOLA V. 为多光谱声学后向散射研究奠定基础。加拿大地质调查局, 公开文件, 2017年, 8295 : 41. <https://doi.org/10.4095/305838>
- [9] CLARKE J. E. H.、DANFORTH B. W. 和 VALENTINE P. 使用95千赫的后向散射角响应进行区域海床分类。“浅水高频声学”会议论文集, 莱里奇, 1997年, 第243-250页。 http://hydrometrica.com/wp/wp-content/uploads/HFSW_1997_Lerici.pdf
- [10] 应用物理实验室。陆军工程兵团-华盛顿大学高频海洋环境声学模型手册。华盛顿大学应用物理实验室, 华盛顿州西雅图, 1994年. <https://staff.washington.edu/dushaw/epubs/APLTM9407.pdf>
- [11] WILSON M. F. J.、O'CONNELL B.、BROWN C.、GUINAN J. C. 和 GREHAN A. J. 多尺度地形分析多波束测深数据用于大陆坡栖息地测绘。海洋大地测量学, 2007年, 30(1-2) : 3-35. <https://doi.org/10.1080/01490410701295962>
- [12] EDWARDS B. D.、DARTNELL P. 和 CHEZAR H. 使用海底摄影和多波束声纳图像表征圣莫尼卡湾的底栖基质。海洋环境研究, 2003年, 56 : 47-66. [https://doi.org/10.1016/S0141-1136\(02\)00324-0](https://doi.org/10.1016/S0141-1136(02)00324-0)
- [13] FONSECA L. 和 MAYER L. 通过将角范围分析应用于多波束声纳数据来远程估计海床特性。海洋地球物理研究, 2007年, 28 : 119-126. <https://doi.org/10.1007/s11001-007-9019-4>
- [14] FONSECA L. E. 和 CALDER B. R. 在角响应空间中聚类声学后向散射。美国水文会议, 2007年, 384. <https://scholars.unh.edu/ccom/384>
- [15] FARIHAH R. A.、MANIK H. M. 和 HARSONO G. 使用多波束回声测深仪技术测量和分析帕卢湾沉积物分类的声学后向散射。热带海洋与技术杂志, 2020年, 12(2) : 437-453. <https://doi.org/10.29244/jitkt.v12i2.28465>
- [16] FAHRULIAN F.、MANIK H. M.、JAYA I. 和 UDREKH U. 多波束回声测深仪数据的角度范围分析(阿拉)和钾均值聚类用于确定沉积物类型。吉拉乌丹 : 印度尼西亚海洋科学杂志, 2016年, 21(4) : 177-184. <https://doi.org/10.14710/ik.ijms.21.4.177-184>
- [17] PRATOMO D. G.、KHOMSIN、CAHYADI M. N.、AKBAR K. 和 APRILIA E. 使用多波束后向散射数据分析海底沉积物分布。马来西亚机械工程学会网络会议, 2018, 177 : 01026. <https://doi.org/10.1051/mateconf/201817701026>
- [18] LAMARCHE G. , & LURTON X. 关于改进和连贯采集和处理海底测绘声纳后向散射数据的建议。海洋地球物理研究, 2018, 39(1) : 5-22. <https://doi.org/10.1007/s11001-017-9315-6>
- [19] GAIDA T. C.、ALI T. A. T.、SNELLEN M.、SIMKOOEI A. A.、VAN DIJK T. A. G. P. 和 SIMONS D. G. 一种使用多频多波束后向散射数据提高海底沉积物声学鉴别能力的多光谱贝叶斯分类方法。地球科学, 2018年, 8(12) : 455. <https://doi.org/10.3390/geosciences8120455>
- [20] BROWN C. J.、BEAUDOIN J.、BRISSETTE M. 和 GAZZOLA V. 多光谱多波束回声测深仪后向散射可作为改进海底表征的工具。地球科学, 2019, 9(3) : 126. <https://doi.org/10.3390/geosciences9030126>
- [21] R2SONIC. 多波束回声测深仪规格, 2020年. <https://r2sonic.com/wp-content/uploads/2020/03/MBES-Spec-US-03-02-2020.pdf>
- [22] BRENNAN C. W. 多光束校准 : 斑块测试。R2Sonic, 2017年. <https://r2sonic.com/wp-content/uploads/2020/03/The-New-Patch-Test.pdf>
- [23] 国际原子能机构。收集和制备用于分析放射性核素

- 和微量元素的底部沉积物样品。国际原子能机构，维也纳，2003年。<https://www.iaea.org/publications/6674/collection-and-preparation-of-bottom-sediment-samples-for-analysis-of-radionuclides-and-trace-elements>
- [24] 雷驰。筛分分析：仔细观察质量。粒度分析专家指南。2015年。<https://www.retsch.ru/files/8785/expert-guide-sieving.pdf?ysclid=lxj4gres950003340>
- [25] FRANCE-LANORD C.、SPIESS V.、KLAUS A.、ADHIKARI R. R.、ADHIKARI S. K.、BAHK J.-J.、BAXTER A. T.、CRUZ J. W.、DAS S. K.、DEKENS P.、DULEBA W.、FOX L. R.、GALY A.、GALY V.、GE J.、GLEASON J. D.、GYAWALI B. R.、HUYGHE P.、JIA G.、LANTZSCH H.、MANOJ M. C.、MARTOS MARTIN Y.、MEYNADIER L.、NAJMAN Y. M. R.、NAKAJIMA A.、PONTON C.、REILLY B. T.、ROGERS K. G.、SAVIAN J. F.、SCHWENK T.、SELKIN P. A.、WEBER M. E.、WILLIAMS T. 和 YOSHIDA K. 地点乌1452。在：FRANCE-LANORD C.、SPIESS V.、KLAUS A.、SCHWENK T. 和探险队354名科学家。孟加拉扇。国际海洋发现计划论文集，354。国际海洋发现计划，德克萨斯州大学城，2016年。<http://dx.doi.org/10.14379/iodp.proc.354.106.2016>
- [26] LURTON X. 和 LAMARCHE G. (编辑) 海底测绘声纳的后向散射测量：指南和建议，2015年。<https://geohab.org/wp-content/uploads/2018/09/BWSG-REPORT-MAY2015.pdf>
- [27] COSTA B. 多光谱声学后向散射：它对海洋栖息地测绘和管理有多大用处？《海岸研究杂志》，2019年，35(5)：1062–1079。<https://doi.org/10.2112/JCOASTRES-D-18-00103.1>
- [28] WANG J.、LI G.、KAN G.、HOU Z.、MENG X.、LIU B.、LIU C. 和 LEI S. 珊瑚砂沉积物中声速和衰减的高频依赖性。海洋工程，2021，234：109215。<https://doi.org/10.1016/j.oceaneng.2021.109215>
- [29] CUNNINGHAM M. 不仅仅是河童系数：一个可以充分表征两个评分者之间评分者间信度的程序。SAS全球论坛论文集，2009年。<http://support.sas.com/resources/papers/proceedings09/242-2009.pdf>
- [30] LANDIS J. R. 和 KOCH G. G. 分类数据的观察者一致性测量。生物统计学，1977年，33：159-174。<https://doi.org/10.2307/2529310>